DOI: 10.1002/ (smtd.201800295)
Review

Bio-inspired plasmonic photocatalysts

*Zhihua Liu, Wan Ru Leow and Xiaodong Chen**

Z. Liu, W. R. Leow, Prof. X. Chen

Innovative Centre for Flexible Devices (iFLEX), School of Materials Science and Engineering, Nanyang Technological University, 50 Nanyang Avenue, 639798 Singapore
E-mail: chenxd@ntu.edu.sg
Webpage: http://www.ntu.edu.sg/home/chenxd/

Keywords: plasmonic photocatalyst, bio-inspired material, bio-templated synthesis, bio-inspired light manipulation

Abstract: The conversion of solar energy to sustainable energy sources is a significant field of study for the relief of the world's energy problems, and among the various strategies developed, semiconductor photocatalysts has received significant attention as a promising candidate due to its attractive efficiency, mild reaction condition and low coast. The enhancement of such photocatalysts with plasmonic materials, by virtue of the Schottky junction and localized surface plasma resonance phenomenon, could facilitate the rapid progress in enhancement of photocatalytic efficiency under visible light irradiation. To further improve photocatalytic efficiency, scientists look to nature for inspiration, culminating in the evolution of complex hierarchical structures in order to fully utilize the potential of solar energy. In the past decade, there has been significant progress in the development of bio-inspired plasmonic photocatalysts, such as antireflective surfaces, three-dimensional photonic structures, and branched structures. This feature article describes the state-of-the-art bio-inspired light manipulation approaches, as well as future challenges in solar energy harvesting by plasmonic photocatalyst.

1. Introduction

The modern lifestyle is heavily supported by fossil fuels; coal, oil and natural gas enabled Industrial Revolution and the subsequent rapid development of the human society. While the current society is characterized by an insatiable thirst of energy, the readily available reserves of fossil fuels are becoming scarce, and the ever-growing use of fossil fuels has also brought about the problem of global climate change.[1] Thus, a common goal of mankind is to find alternative energy sources that are also sustainable. There are more than one candidates of new potential energy sources that are renewable, or at least carbon neutral, such as nuclear, hydro, wind, tidal, and solar energies. Among them, solar energy is more scalable and poses less dangers (as compared with public safety concerns of nuclear and hydroelectric energies) during large installation and local energy harvesting. We are now in an era of "solar opportunity", in which free, renewable, carbon-free power is undergoing rapid advancement.[2]

Nature has already taken advantage of solar energy for billions of years; plants, algae, and even some bacteria and animals can transform sunlight into energy-dense carbohydrates via photosynthesis. To mimic the photosynthesis process, a large variety of artificial photocatalyst have been developed.[1, 3] Among them, semiconductors with the appropriate band gap width can capture photons by electron-hole separation between their valence and conduction bands, thus generating the power to drive chemical reactions, such as degrading organic compounds[4] and water splitting. Since the pioneer work reported by Fujishima & Honda[5] using TiO_2 photoanode for water splitting, several families of semiconductor have been investigated.[6, 7] However, large scale application remains rare, as such electrodes still suffer from the intrinsic problem of poor visible light response.[8] The main reason of this problem is high-performance photocatalyst always have large band gap, such as TiO_2 and ZnO_2, only ultraviolet (UV) can be absorbed. As the solar energy in UV region is quite limited, artificial light sources will be necessary to keep the performance of photocatalyst, which making it less attractive. To solve this problem, many groups have reported some novel visible light driven photocatalysts, such as simple oxides (Bi_2O_3[9] and WO_3[10]), sulfides CdS[11], complex oxides (Bi_2WO_6[12]) and metal free catalyst (C_3N_4[13]). But they are still suffering with some problems, especially short electron-hole pair lifetime caused by recombination and limited absorption ability in visible light region. Plasmonic photocatalyst come into focus as a promising technique for fabrication high-performance visible light driven photocatalyst because it can give solution to those problems.[14-19]

Plasmonic photocatalyst involves dispersion the plasmonic active chemical moieties, such as Au, Ag nanoparticles or graphene,[20] into semiconductor photocatalysts. Compared with traditional semiconductor photocatalyst, two distinct features needed to be emphasized, Schottky junction and localized surface plasma resonance (LSPR). Coming to the details about the classical semiconducor photocatalyst, the photons absorbed inside the photocatalyst will generate excited electrons and holes, which will migrate to the surface to initiate chemical reactions. In a homogeneous semiconductor crystal, the migration is a random walk and thus the excited electrons and holes have plenty of chance to recombine, causing low photocatalytic efficiency. By introduction of noble metal directly contact with the semiconductor phoptcatalyst, Schottky barrier, which is an internal electric field in between noble metal and semiconductor junction, is generated in the complex nanoparticle system.[21] Thus, when the electron and hole in photocatalyst separated under the excitation of absorbed photons, they will migrate to different direction under the help of this electric field, which could effectively prolong lifetime of highly reactive electron and hole and further facilitate chemical reactions.

The other feature of so called LSPR is based on the strong oscillation of free electron near metal surface and electric field of incident light.[22] This optical response of noble metal nanoparticles have been well understood and reported.[23] For conciseness, here we pick up the main issues closely related with photocatalyst. From the dynamics of LSPR, the coherent oscillation of electrons dissipates the energy by radiative decay (low efficiency in plasmonic photocatalyst system)[24] and non-radiative decay, which cascaded steps of improved photocatalytic efficiency caused by electron-electron and electron-phonon relaxation.[25] In the volume of metal nanoparticles, the electron states are continuously filled under the Fermi energy level (E_f), following the Fermi-Dirac distribution. Under the irradiation of photons, resonance electrons will collect energy to the energy level higher than the conduction band (E_{CB}) of neighboring semiconductor. This will facilitate a direct transfer of electrons to the conduction band of semiconductor (energy diagram of **Figure 1**).[26] The other process of electron–phonon relaxation refers to the collision of electrons with the ionic lattice of the metal nanoparticles. This will cause an localized heating effect in the metal nanoparticles.[27] Through the heating process does not produce active electrons or holes, it can be used for thermolysis and also beneficial to photocatalysis because photochemical reactions go faster at a higher temperate. Further more, the LSPR itself can also give molecule polarization effect, enhanced local electric field[19] and the absorbance band can be tuned by particle size, dielectric environment and aggregation to fit the broadband absorption demands of semiconductor photocatalyst.[28, 29]

The research on pursuing efficient, robust and low cost plasmonic photocatalysts not only carried on fundamental components design, but so on photo-harvesting step. By optimizing structures of photocatalyst, more photons can be absorbed to generate electron-hole separation and further improving photocatalytic efficiency.[30] In fact, efficient light harvesting are of fundamental importance to biological systems for their survival. After millions year's evolution, nature already give remarkable examples of optical structures that render unique and well-defined optical properties through efficient manipulation of light through absorption, reflection, scattering, diffraction, interference, and even combinations several of these effects.[31] Learning, inspiring and mimicking from nature and applying nature's engineering principles combining with plasmonic effect is a promising approach to develop high efficient photocatalyst. Here, we review this exciting and developing area namely bio-inspired plasmonic photocatalyst. In this feature article, we will focuses on the recent progress in rational design, fabrication and application of plasmonic photocatalyst inspired by bio-structures such as antireflective, bio-photonic, biomorphic structures and bio-compounds assisted fabrication procedures, while providing perspective on the future development of this area.

2. Bio-structure inspired plasmonic photocatalyst

Light is the basis of all life on our planet. After million year's evolution, most organisms on earth have evolved to utilize light in their own way by numerous delicate hierarchical structures ranging from nano to macro scale, giving unique and wonderful properties to them.[32] As one of the best example, butterfly's wings with diverse brilliant colors have typical hierarchical periodic architectures, which exhibit an inherent multifunctional integration.[33] The structures of compound eyes, such as dragonflies, could provide a very large view-angle, and can detect fast movement by more than 30,000 lenses each.[34] More interestingly, compound eye of some kinds of shrimps could achieve polarized vision.[35] Inspiration form those unique hierarchical architectures could broaden the horizon for the design of high efficient photocatalysts and provide working prototypes to exploit solar energy.

2.1. Anti-reflective structure inspired plasmonic photocatalyst

Many natural systems are able to use nano scale architectures to achieve high light utilization with limited reflection, such as moth eye (**Figure 2**a, b),[36, 37] glasswing butterfly[38] and cicada's wing (Figure 2c, d).[39] The antireflective bio-structure normally composed by sub-wavelength sized nanoarray that provides a gradient in refractive index suppressing the light reflection and increasing transmission at the surface towards a large range of wavelengths and incident angles.[40] Inspired by the structures from those insects, lots of nanostructure arrays have been developed as antireflective coatings or surfaces, and get further aplication to improve performance of solar cell,[41] light emitting diode, *et al*.[42]

To combine the advantage of bio-inspired antireflective surface and plasmonic photocatalyst, Chen's group reported a novel method to fabricate composite film of honeycomb graphene oxide (GO) films covered by ZnO nanorods (NRs).[43] The film is fabricated by evaporation cooling induced self-assembly of GO/DODA (dimethyldioctadecylammonium),[44-46] following with in situ reduce and hydrothermal growth of ZnO nanorods (NRs) (Figure 2e). Compared to the smooth film of ZnO NRs on reduced GO/DODA, the honeycomb film of ZnO NR coated film demonstrated a decrease of 26% on incident light reflection (Figure 2f) and hence, a three-fold increase of photocurrent generation compared with plane structure was achieved (Figure 2g). This is a highly feasible approach to significantly improve the photoelectric conversion efficiency of a ZnO photoanode.

To fabricate antireflective surface, pillar array is a widely used structure.[40, 47] Among large variety of selectable materials, silicon has a bandgap of 1.12 eV, which is excellent for capturing photons in the red part of the solar spectrum. Taking the advantage of low-cost and chemical stability of scalable chemical vapor deposition, Chorkendorff and co-worker reported bio-inspired molecular clusters (Mo_3S_4) loaded on silicon nanopillar array for efficiently catalyzing the evolution of hydrogen.[48] The plasmonic photocatalyst they fabricated could obtain current density at the reversible potential is sufficient for use in a 10% solar-to-hydrogen efficiency. As a typical method, nanoarray structure made by gold nanorods are also served as light-harvesting antennae to facilitate water splitting of TiO_2 under visible light irradiation.[49, 50]

2.2. 3D photonic structure inspired plasmonic photocatalyst

Fascinating biological 3D photonic structures are ancient, having first evolved millions of years ago. They are also used as analogous/models to the synthetic photonic crystal that created in laboratory.[51] Sever example of biological 3D packed photonic structure have been discovered in beetles, such as face-centered cubic structure of longhorn *Pseudomyagrus* *waterhousei* (**Figure 3**a) that gives a colorful blue-violet color (Figure 3b),[52] and *Pachyrrhynchus congestus pavonius* given a orange color (Figure 3c, d).[53] Comes to details of those interesting color. When light enters photonic crystals, a specific waveband of light can be trapped because of multireflection. Besides, the spatial structures can produce coherent Bragg diffraction that prevents light with frequencies in the stop band from passing through the material, which is called slow photons effect.[54] When the slow photon wavelength overlaps with the light that the material can absorb, an enhanced light absorption can be obtained.[30, 55]

Inspired from biological photonic structure, plasmonic photocatalyst light harvesting enhancement can be achieved by adopting appropriate 3D photonic structures. Under the guideline of this methology, Majima and co-workers prepared a 3D-array of monodispersed gold nanosphere (AuNS) and TiO_2 yolk-shell nanosphere (Au-TiO_2) as plasmonic photocatalyst.[56] They used AuNS as core and coated two layers of SiO_2 one layer as the template and another as protector to protect the TiO_2 layer inbetween SiO_2 during calcining (**Figure 4**a). Then, SiO_2 layers were removed by NaOH etching (Figure 4b). The subsequent hollow Au-TiO_2 acted as building blocks for fabricating unique 3D assembled array of Au-TiO_2 3D photonic structure(Figure 4c), which was applied as plasmonic photocatalyst for H_2 generation. Compared with TiO_2 hollow structure, Au-TiO_2 exhibited significantly promoted photocatalytic activity (3-4 fold higher). It is because the nearly close packed Au-TiO_2 gives rise to enhanced multi-scattering and these scattered light can transfer to the neighboring Au-TiO_2, which causes longer optical paths length of incident light in 3D-array. Therefore, the scattering light greatly increases the chance of AuNS to absorb light. As is discussed before, the Schottky barrier will be formed once metal contact with semiconductor, if the Au NS location moved from center to the shell of the hollow sphere, the photocatalytic efficiency can be improved than pure TiO_2 also. This hypothesis is proved by Do's work.[57] They reported hollow Au-TiO_2 3D structure, but Au nanoparticles is located at the shell, which is thin-shell Au/TiO_2 hollow nanospheres (Au/TiO_2-3DHNSs). Titanate nanodisks (TNDs) and polyelectrolyte deposited in layer-by-layer way on SiO_2 nanoshperes (Figure 4d). Then this nanosphere absorbed $AuCl_4^-$ and assembled into 3D ordered opal structures following with calcining and removing SiO_2 core (Figure 4e, f). The as prepared Au/TiO_2-3DHNSs showed 6.1 times higher photocatalyst ability than pure Au/TiO_2-P25 under the same visible light irradiation. The enhancement is attributed to the photonic nanostructure related photonic band edge matched with wavelength Au SPR absorption.

Besides hollow sphere assembled opal 3D photonic structures, inverse opal structure fabricated by template synthesis could facilitate visible light absorption of plasmonic photocatalyst also. Jang and co-workers investigated this structure by surface-textured TiO_2 coated with gold nanoparticle (Au/st-TIO) plasmonic photocatalyst.[58] The photocatalyst is fabricated by a commonly used self-assembly of polystyrene (PS) beads following with infiltrating of TiO_2 precursor $TiCl_4$. After the sol-gel reaction and calcinations, PS part can be selectively removed to generate inverse opal structured TiO_2. To load gold nanoparticles, they deposited the Au NP with diameter of 30 nm on the 3D textured TiO_2 (**Figure 5**a). Compared with bare TiO_2 catalyst, Au/st-TIO exhibit a maximum of 2.86 times higher photocurrent density (Figure 5b). This enhancement is coming from strong and broad absorption band ranging from 400 to 800 nm, which is due to scattering provided by the interval opal structure combined with plasmonic effect of gold nanoparticles. The inverse opal structure via template synthesis is quite universal, it can be easily expand to other compounds. Baumberg *et al* reported this structure fabricated by small band gap visible-light-driven photocatalyst $BiVO_4$ (bandwidth 2.4 eV) and gold nanoparticle.[59] They prepared the io-Mo:$BiVO_4$ films from colloidal crystal templates of PS with 260 nm and 320 nm diameter (Figure 5c, d). By tunning the size of template PS sphere, the photonic stop bands of synthesized io-Mo:$BiVO_4$ films are controlled to located at 510 nm and 580 nm respectively. The plasmonic effect of Au NPs can be significantly amplified in the inverse opal structure prepared by 260 nm PS sphere due to a strong coupling with the photonic Bragg resonance and hence 4 times higher photocurrents than equivalent planar electrodes achieved (Figure 5e). To further take advantage of slow photon effect of photonic crystal, Kang and co-workers reported TiO_2 bi-layer structure in which a template-assisted photonic crystal covered on a vertically oriented TiO_2 nanotube layer.[60] Other combined structure such as well-ordered porous nanostructure on top of a uniform TiO_2 nanotube array[61], and ternary nanocomposite of Au-decorated Bi_2MoO_6 nanosheet/TiO_2 nanotube array hetero structure[62] are introduced for photonic crystal assisted plasmonic photocatalyst. This method gives a new perspective of constructing structures for efficient light utilization.

2.3. Biomorphic branching structure inspired plasmonic photocatalyst

Natural hierarchical structures of branch given direct help on highly efficient photosynthetic process. Tree's branches are stretching out as far and wide as possible to help the leaves reach light as much as possible. This branches also help a tree to have more leaves than just grew directly from trunk. Inspired from this structure, vertically oriented branches already offered an excellent material architecture for photovoltaic applications due to their unique merits such as lower carrier recombination loss, decoupling directions of light absorption, charge-carrier collection and vectorial charge carrier transport perpendicularly to the charge collecting substrates.[63]

3D branched structure in nano scale are also introduced to plasmonic photocatalyst because of its higher carrier generation and separation ratio, higher specific surface area, higher organic pollutant absorption, faster charge transport, and superior light-harvesting efficiency for efficient charge collection. [64, 65] To further taking the advantage of plasmonic effect assisted photocatalyst, Kang and co-worker constructed 3D branched ZnO nanowire arrays (B-ZnO NWs) decorated by gold nanoparticles photocatalyst.[66] They grew a layer of single crystal ZnO NWs on FTO substrate, then the outside layer ZnO is converted to polycrystalline state by ion-exchange to ZnS and annealing in air. Second-generation ZnO NWs growth was seeded by the outside layer ZnO (Figure 6a). Gold nanoparticles are loaded on all of the branches by wet chemical reaction which could avoid the shadow effect of vacuum evaporation (Figure 6b). The B-ZnO NWs exhibited clear improvement of photocatalyst activity compared to the non branched P-ZnO NWs (Figure 6c). This improvement was ascribed to the enhanced light capturing ability and the increased semiconductor/liquid interfaces which was benefit for charge transport and chemical reaction. Similar branched structure also applied to anatase/rutile mixed-phase TiO_2 hierarchical network deposited with gold nanoparticles, which was reported by Yen *et al.*.[67] Plasmonic silver nanoparticle assisted plasmanic photocatalyst of 3D pine tree-like hierarchical TiO_2 nanotube array is fabricate and investigated by Xiao and co-worker.[68] composite Ag/TiO_2-branched nanotube arrays they fabricated shown outstanding photocatalytic property.

To make the synthesis of 3D branched structure easier, Bi and co-worker present a facile and general growth route single-step synthesis of AgCl nanoplate-Ag/AgCl nanowire hierarchical heterostructures.[69] The Ag nanowires fabricated by a modified polyol process was serve as the starting templates. The Ag nanowires were oxidized by $CuCl_2$ at room temperature to generate hierarchical branched structure (Figure 6d,e). Thus fabricated AgCl based photocatalysts exhibit excellent photocatalytic activities for the RhB degradation compared with commercial N-doped TiO2, and Ag nanowires (Figure 6f).

Not only hard branched structure form tree and leaves, scientist get inspiration from flexible hair-like structure of cilia to fabricate similar structures to manipulate fluids on the micro scale.[70] Xu and co-worker assembled an inner-motile magnetically actuated artificial cilia film into the photocatalytic hydrogen production system of TiO_2.[71] They further developed this technique to the inner-motile branched ZnO nanowires arrays with CdS quantum dots.[72] The film they prepared exhibit dramatically enhanced photocatalytic water splitting capability due to the timely desorption of H_2 and the performance can be controlled with adjusting the actuation frequency of rotational magnetic fields.

3. Biomaterial assisted plasmonic photocatalyst

Many of the biomaterials nature uses to create its special biological systems and functions are themselves very attractive for future application. One reason that biomaterials are of interest is their delicate hierarchical structure which can be replicated by artificial method only in very complicated, noneconomic or even non environmental friendly way. Another reason is many of these biomaterial are easily obtainable on large scales and their biological compatibility. Large verity of biomaterials are used to assist synthesis nanomaterial including photocatalyst.[73] Based on the scale of biomaterial candidates, bio-inspired syntheses can be divided into two different types. First, biometrics with sizes ranging from nanometers and microns to macro scale, such as inset wings,[39, 74, 75] plants leaves[76, 77] and viruses.[78] Second, biomolecules secreted,extracted or inpired from microorganisms and plants such as DNA,[79] proteins[80] chitin,[81] silk[82-85] and biosilica.[86]

3.1. Butterfly wing based periodic porous template

The scale of hierarchical structures of biologic system responsible for bio-optical function can be on the order of only a few nanometers up to hundreds of nanometers and incorporated in even larger structures up to micron and mm scale. It is a ongoing desire to replicate the intricate details from biologic system by artificial way. However, fully copy this hierarchical structure is quite challenge for direct artificial top-down or bottom-up way. Biotemplating is one faithful method to reproduce biological structures.[87-89] In this method, two different direction can be adopted for the replication of biological structure. One way is infiltrate artificial compounds to the biological molds, after the removal of original molds, inverse structure can be made.[89] This way can only apply to open architectures. The other way is absorb precursor into the porous architecture following with sol-gel or calcinations to get a fully replica of the original structure.[74]

Butterflies are universally attractive because of their colorful wings, which is resulting from their elaborate 1D, 2D, or 3D photonic crystal structures.[33, 90] *Papilio Paris* wings exhibit high light-harvesting ability in black areas (Figure 7a).[91] The ridging and the periodic porous structure in the dark areas are responsible for the light-harvesting of the wings by increasing the optical path length (Figure 7b, c).[92] Inspired by this structural features, Zhang *et al.* prepared Au/TiO_2 nanocomposites through sol-gel technique in ethanol/water medium followed deposition-precipitation process, using butterfly wings as the template.[93] Compared with original template butterfly wings, the replicate preserved the complicated reticular structure, which exhibited a cavity diameters comparable with the wavelength of visible light about 400-800 nm (Figure 7d, e). The synthesized biomorphic Au/TiO_2 with gold to titanium of 8 wt% shows almost two times improved photocatalytic activity on methyl orange degradation than pure TiO_2 particles. This strategy provided an effective way for the synthesis of high performance plasmonic photocatalysts, and it could extend to other types of devices by involving analogous bio-functional structures.

Inspired by the photosynthesis center in natural leaves and 3D structure of butterflies utilizing solar energy through combination of components and structure, Fan and co-workers synthesized CdS/Au/TiO_2 three components photocatalyst, using the wings of butterfly *Papilio nephelus Boisduva* as template.[94] TiO_2 and CdS mimetic function of photosynthesis center II and I,[95] Au acts as plasmonic electron mediator. They fund under the help of wing architecture, CdS/Au/TiO_2 shown improved water-splitting efficiency by 2 times compared to the TiO_2 with plate architecture. To further explore the photocatalyst in red-to-IR region, this they demonstrated a new strategy, which adopted nature's far red-to-NIR responsive architectures for an efficient bio-inspired photocatalytic system.[96] The photocatalyst is fabricated by a typical visible light responsive photocatalytic Bismuth vanadate (BVO),[97, 98] through sol-gel method, using a series of different butterfly wings as template (Figure 8a). Inside the pores of artificial wing, plasmonic nanoantennas of gold nanorods which had tunable SPR absorption band were assembled, driving by electrostatic interaction (Figure 8b). The artificial wing (Figure 8c) shown up to 25% enhanced red-to-NIR (700~1200 nm) harvesting, and enhanced electric-field amplitude of LSPR to more than 3.5 times than that of the non-structured one (Figure 8d, e). To give a short summarize, those improved photocatalystic efficiency is mainly attribute to the 3D wing structure which tends to enhance optical absorption and magnify the LSPR-induced electric field, that further promote electron-hole separation, thus improving the photocurrent generation.[96]

3.2. Plant Leaves based porous template

Green leaves of plants play a fundamental role in the natural life cycle. Leaves posses elaborated structures and functional components to produce a highly complex machinery for photosynthesis. In leaves, light harvesting, photo-induced charge separation, and catalysis modules combined together to efficiently capture solar energy and store it to chemical compounds.[99] To support photosynthesis, green leaves are designed by nature to be masters of light harvesting with different microstructures of vessels and fibers that are responsible for mechanical strength and also the distribution of water and nutrients to the photosynthetic cells (Figure 9a).[100] These vascular bundles are rich in lignin which can work as a hierarchical porous morphology skeleton after removing softer tissue surrounding the vessels, making leaves particularly well-suited as a template for photocatalyst.[101-103]

To fully replicate the structure of leaves is a challenge because they have delicate but physically weak structures, normal way of filtration not working on this system. To issue this problem, using green leaves as templates, Fan and co-worker developed a general method to fabricate semiconductor photocatalyst by two-step infiltration method.[104] Template leaves were treated with a dilute HCl solution to replace K, Ca, P and S ions and Mg ions in the porphyrins of the chlorophyll molecules by H^+. Then, the as-treated leaves were stressed with

$TiCl_3$ solution first time, with Ti ions being introduced into the tissues to replace the H^+ in the pheophytins. Second sol-gel infiltration with tetrabutyl titanate ($Ti(OBu)_4$)/ethanol to coat the cuticles and the cell walls of the vascular bundles, bundle sheaths and mesophyll, which are mainly composed of cellulose, hemicellulose and lignin. The infiltrated samples were desiccated and calcined to get rid of the templates and crystallize the morph-TiO_2. Under the help of this method, they developed photocatalytic system combined leave template based morphology with plasmonic gold nanoparticles components.[105] The incorporated photocatalytic modules CdS(shell)/Au(core)/N-TiO_2 was prepared by *Cherry blossom* leaves as template (Figure 9b). The replicas inherit the hierarchical morphologies of the natural leaf at macro, micro, and nanoscales including a porous framework of veins (Figure 9c, d). Such hierarchical porous morphologies endow them with high specific surface areas and macropore/mesopore architectures. The H_2 evolution rates of optimized CdS/Au/N-TiO_2 three-component hetero structures are about 2.6 times of N-TiO_2 under UV/visible light, and about 270 times of Au/N-TiO_2under visible light irradiation.

By applying similar strategy, Ye and co-workers demonstrated 3D artificial photosynthesis architecture as an efficient mass flow network for improved gas diffusion and light harvesting relying on the morphological replacement of leafs 3D hierarchical architecture into perovskite titanates.[106]

Not only working as framwork, the leaves could be used as sources of dopant or reductant reagent for synthesis of nanoparticle or semiconductors. Xie and co-workers emploied bamboo leaves as template to synthesis ternary composite of Ag/CN-TiO_2@g-C_3N_4 photocatalyst.[107] The C/N dopant were come from the elements in leaves tissue.

3.3. Bio-compounds assisted plasmonic photocatalyst

Metal nanoparticles are key components for plasmonic photocatalyst. Normally metal nanoparticles are synthesized by solution based bottom-up method using toxic compounds as precursor, or evaporation method where complicated equipment will be involved. However, in natural environments, some metal ions could be adsorbed and further reduced to elemental metals by microorganisms, plants, biomass under mild condition.[108-110] Inspired by the biological formation of metal nanoparticles, bio-compounds syntheses have emerged as innovative fabrication for plasmonic photocatalyst. Rege and collegues exploit the microfluidics as well as compounds of processed Magnolia leaves’ vasculature to template the in situ generation of plasmonic metal (gold and silver) nanoparticles for photocatalystic reaction of *p*-nitrophenol to *p*-aminophenol.[77]

Normal nanoparticle synthesis need harsh reaction conditions, such as high temperture strong acid or base chemical, and even high presure. Biogenic technology using bacteria or other microorganisms usually occur at ambient pressure and temperature with a lower environmental impact. Recently, Liu and co-workers reported a facile synthetic protocol for producing small plasmonic Ag@AgCl plasmonic catalyst in microbe-free lysogeny broth (LB) under mild conditions.[111] In this stady, stable AgCl colloidal spheres with a size of 50 nm were formed through a precipitation reaction of $AgNO_3$ and NaCl in LB Miller broth. LB contains yeast extract and peptone that are rich in amino acids and peptides. Ag nanoparticle can be generated by laser irradiation on AgCl assisted by peptide mediated electron transfer (Figure 10a).[112] By rationally changing the precursor concentration and light exposure time, they could finely tune the bandgap of the composites. They further combining this method with Kirkendall effect (the ion-exchange reaction between Br^- and AgCl due to the large difference between the solubility of AgBr and AgCl) to synthesis hollow Ag@AgBr nanospheres. The nanospheres shown excellent solar light-induced oxidizing properties against both microbial and chemical contaminants.[113] This method opened a new opportunity for the development of more advanced Ag@AgX-based photocatalysts to address energy conversion, green chemistry, and meet the environmental demands for the future.

Mussels are promiscuous fouling organisms and have been shown to attach to virtually all types of inorganic and organic surfaces even classically adhesion-resistant materials such as poly(tetrafluoroethylene). Mussels' adhesive versatility origin from the amino acid composition of proteins found near the plaque-substrate interface, which are rich in 3,4-dihydroxy-L-phenylalanine (DOPA).[114] As a mimicry of mussel adhesive proteins, polydopamine (PDA) coating was developed to coat wide variety of material surfaces and allows facile synthesis of various functional nanostructures.[115] Recently, Park and colleague created core-shell nanohybrid assemblies for plasmon-enhanced photocatalyst, using PDA as building component.[116] The PDA compound played multirole in this photocatalyst system: a reducing agent for plasmonic metal deposition, a scaffold for Eosin Y (EY) dye encapsulation, and an adhesive layer between nanohybrid and substrate (Figure 10b). This approach is material and morphology independent, they film can be fabricated on different substrates, such as slide glasses, flexible PET films, and silica beads (900 nm in diameter) (Figure 10c). The plasmon-derived enhancement was demonstrated in the enzymatic photosynthesis of L-glutamate by L-glutamate dehydrogenase coupled with the photochemical nicotinamide cofactor (NADH) regeneration. This strategy can be expand to Au-TiO_2 photocatalyst system also, Huo and co-workers synthesized a catalytic nanocomposite membrane, introducing Au-TiO_2 onto PVDF membrane for degrading of tetracycline.[117]

Inspired by the biomineralization process, where complex architecture is achieved via polyamine-mediated mineralization and assembly,[110] Rana and co-worker demonstrate the synthesis of rGO-ZnO[118] nanostructures GO-Ag/AgCl[119] in a single step using polyamines. which simultaneously facilicate the interaction between semiconductors and graphene oxide to achieve enhanced photocatalytic activity via effectively separation of photoinduced carriers.

4. Conclusions and Perspectives

Nature comprises highly complex and sophisticated engineering models ranging from the nano- to macroscale for efficient light manipulation. Based on bio-inspiration, which involves learning from the design principles in nature, many strategies for the effective enhancement of photocatalytic efficiency were developed, such as photonic, multiscale hierarchical structures and bio-inspired plasmonic photocatalyst. However, the efficiency remains too low to replace fossil fuels industrial applications.[120] Not only that, even though the developed bio-inspired photocatalysts continually improves in terms of efficacy and sophistication, we have only just scratched the surface of nature.[51] There exists more undiscovered biosystems in nature than that which have been explored and understood. Scientists need to delve deeper to find more interesting but yet explored systems, and, in conjunction with breakthroughs in materials synthesis techniques, fabricate novel nanomaterials with great capability for light manipulation.

Not only that, it is believed that the combination/hybridization between non-biological nanocompounds and biologic organelles may also have the potential to impart organelles with new and enhanced functions. Some pioneering work have already conducted in this direction. For instance, Strano and coworker introduced single-walled carbon nanotubes through passive transport and irreversible localization within the lipid envelope of extracted plant chloroplasts.[121] The as-prepared hybrid photosystem is endowed with photosynthetic activity that is over three times higher than the original activity, as well as enhanced electron transport rates. Yang and colleagues used biologically-precipitated cadmium sulfide nanoparticles as the light harvester to sustain cellular metabolism;[122] a nonphotosynthetic bacterium, *Moorella thermoacetica*, was made to photosensitize itself with cadmium sulfide nanoparticles, which enabled the photo-production of acetic acid from carbon dioxide at relatively high quantum yields over several days of light-dark cycles. This strategy of incorporating artificial nanomaterial with living systems could expand the material library available, providing one more alternative for light absorption to raise the upper limit on the efficiency of artificial photosynthesis.

Fundamentally, to increase the generation efficiency of excited electrons, it is important to have a rational design of plasmonic photocatalysts. Precise control of the components arrangement on the plasmonic metal surface itself and at the interface between the plasmonic metal and the semiconductor should be investigated to prevent the recombination of electron–hole pairs, and to increase the hot electron injection efficiency, which triggers and boosts the chemical reaction. To achieve this, Chen's group developed photocatalyst with designable energy band structure and tunable heterogeneous interfaces along the axial direction of 1D nanobamboo architectures (NBA) of CdS-Au[123] and ZnS-Ag-CdS-Au-CdSe[124] by hard-template-assisted electrochemical deposition.[125] The energy band structure and heterogeneous interfaces are shown to be exquisitely engineered in these NBA architectures to attain optimal charge separation and transportation. This method give the possbility to programmable cooperation of unique physical and chemical properties of each component allows these smart architectures to possess excellent synergistic performance in enhancing the solar-to-chemical energy conversion efficiency.

Last but not least, bio-inspired plasmonic photocatalyst is an extremely multidisciplinary field. Biologists, physicists, chemists, material scientists and engineers all play important role in this rapid developing field. New insights, new understanding and new tools often emerge at the intersections between these disciplines. In order to successfully develop photocatalysts suitable for large-scale application, we need to break barriers and build bridges between disciplines.

Acknowledgements

The authors thank the financial support from Singapore Ministry of Education (MOE2014-T3-1-004 and MOE2014-T2-2-140).

Received: ((will be filled in by the editorial staff))
Revised: ((will be filled in by the editorial staff))
Published online: ((will be filled in by the editorial staff))

References

[1] J. Barber, P. D. Tran, *J. R. Soc. Interface* **2013**, 10, 20120984.
[2] N. S. Lewis, D. G. Nocera, *Proc. Natl. Acad. Sci. U. S. A.* **2007**, 104, 20142.
[3] X. Lang, X. Chen, J. Zhao, *Chem. Soc. Rev.* **2014**, 43, 473.
[4] X. Lang, J. Zhao, X. Chen, *Chem. Soc. Rev.* **2016**, 45, 3026.
[5] A. Fujishima, K. Honda, *Nature* **1972**, 238, 37.
[6] M. R. Hoffmann, S. T. Martin, W. Choi, D. W. Bahnemann, *Chem. Rev.* **1995**, 95, 69.
[7] J. M. Herrmann, *Catal. Today* **1999**, 53, 115.
[8] K. Hashimoto, H. Irie, A. Fujishima, *Jpn. J. Appl. Phys., Part 1* **2005**, 44, 8269.
[9] L. Zhang, W. Wang, J. Yang, Z. Chen, W. Zhang, L. Zhou, S. Liu, *Applied Catalysis A: General* **2006**, 308, 105.
[10] D. Chen, J. H. Ye, *Adv. Funct. Mater.* **2008**, 18, 1922.
[11] N. Bao, L. Shen, T. Takata, K. Domen, *Chem. Mater.* **2008**, 20, 110.
[12] L. Zhang, W. Wang, Z. Chen, L. Zhou, H. Xu, W. Zhu, *J. Mater. Chem.* **2007**, 17, 2526.
[13] X. Wang, K. Maeda, A. Thomas, K. Takanabe, G. Xin, J. M. Carlsson, K. Domen, M. Antonietti, *Nat. Mater.* **2009**, 8, 76.
[14] K. Awazu, M. Fujimaki, C. Rockstuhl, J. Tominaga, H. Murakami, Y. Ohki, N. Yoshida, T. Watanabe, *J. Am. Chem. Soc.* **2008**, 130, 1676.
[15] H. Cheng, T. Kamegawa, K. Mori, H. Yamashita, *Angew. Chem. Int. Ed. Engl.* **2014**, 53, 2910.
[16] Y. X. Tang, Z. L. Jiang, G. C. Xing, A. R. Li, P. D. Kanhere, Y. Y. Zhang, T. C. Sum, S. Z. Li, X. D. Chen, Z. L. Dong, Z. Chen, *Adv. Funct. Mater.* **2013**, 23, 2932.
[17] S. Linic, P. Christopher, D. B. Ingram, *Nat. Mater.* **2011**, 10, 911.
[18] H. Wang, L. Zhang, Z. Chen, J. Hu, S. Li, Z. Wang, J. Liu, X. Wang, *Chem. Soc. Rev.* **2014**, 43, 5234.
[19] X. Zhang, Y. L. Chen, R. S. Liu, D. P. Tsai, *Rep Prog Phys* **2013**, 76, 046401.
[20] Q. Xiang, J. Yu, M. Jaroniec, *Chem. Soc. Rev.* **2012**, 41, 782.
[21] R. T. Tung, *Phys. Rev. B* **2001**, 64.
[22] S. A. Maier, *Plasmonics: Fundamentals and Applications*, Springer US, **2010**.
[23] S. A. Maier, **2007**, DOI: 10.1007/0-387-37825-1.
[24] E. Dulkeith, T. Niedereichholz, T. Klar, J. Feldmann, G. von Plessen, D. Gittins, K. Mayya, F. Caruso, *Phys. Rev. B* **2004**, 70.
[25] S. Link, M. A. El-Sayed, *J. Phys. Chem. B* **1999**, 103, 8410.
[26] Y. Nishijima, K. Ueno, Y. Yokota, K. Murakoshi, H. Misawa, *J. Phys. Chem. Lett.* **2010**, 1, 2031.
[27] C. K. Sun, F. Vallée, L. H. Acioli, E. P. Ippen, J. G. Fujimoto, *Phys. Rev. B* **1994**, 50, 15337.
[28] C. Liow, F. Meng, X. Chen, S. Li, *J. Phys. Chem. C* **2014**, 118, 27531.
[29] K. L. Kelly, E. Coronado, L. L. Zhao, G. C. Schatz, *J. Phys. Chem. B* **2003**, 107, 668.
[30] S. Lou, X. Guo, T. Fan, D. Zhang, *Energ. Environ. Sci.* **2012**, 5, 9195.
[31] S. Tadepalli, J. M. Slocik, M. K. Gupta, R. R. Naik, S. Singamaneni, *Chem. Rev.* **2017**, 117, 12705.
[32] H. Zhou, J. Xu, X. Liu, H. Zhang, D. Wang, Z. Chen, D. Zhang, T. Fan, *Adv. Funct. Mater.* **2018**, 28, 1705309.
[33] R. O. Prum, T. Quinn, R. H. Torres, *J. Exp. Biol.* **2006**, 209, 748.
[34] M. F. Land, D. E. Nilsson, *Animal Eyes*, Oxford University Press, **2002**.
[35] P. C. Brady, A. A. Gilerson, G. W. Kattawar, J. M. Sullivan, M. S. Twardowski, H. M. Dierssen, M. Gao, K. Travis, R. I. Etheredge, A. Tonizzo, A. Ibrahim, C. Carrizo, Y. Gu, B. J. Russell, K. Mislinski, S. Zhao, M. E. Cummings, *Science* **2015**, 350, 965.

[36] C. G. Bernhard, W. H. Miller, *Acta Physiol. Scand.* **1962**, 56, 385.
[37] D. G. Stavenga, S. Foletti, G. Palasantzas, K. Arikawa, *Proc. Biol. Sci.* **2006**, 273, 661.
[38] R. H. Siddique, G. Gomard, H. Holscher, *Nat. Commun.* **2015**, 6, 6909.
[39] Y. F. Huang, Y. J. Jen, L. C. Chen, K. H. Chen, S. Chattopadhyay, *ACS Nano* **2015**, 9, 301.
[40] J. Cai, L. Qi, *Mater. Horiz.* **2015**, 2, 37.
[41] L. Chan, D. Kang, S.-M. Lee, W. Li, H. Hunter, J. Yoon, *Appl. Phys. Lett.* **2014**, 104, 223905.
[42] J. J. Kim, Y. Lee, H. G. Kim, K. J. Choi, H. S. Kweon, S. Park, K. H. Jeong, *Proc. Natl. Acad. Sci. U. S. A.* **2012**, 109, 18674.
[43] S. Yin, X. Men, H. Sun, P. She, W. Zhang, C. Wu, W. Qin, X. Chen, *J. Mater. Chem. A* **2015**, 3, 12016.
[44] S. Yin, Z. Niu, X. Chen, *Small* **2012**, 8, 2458.
[45] S. Y. Yin, Y. Goldovsky, M. Herzberg, L. Liu, H. Sun, Y. Y. Zhang, F. B. Meng, X. B. Cao, D. D. Sun, H. Y. Chen, A. Kushmaro, X. D. Chen, *Adv. Funct. Mater.* **2013**, 23, 2972.
[46] D. Qi, L. Zheng, X. Cao, Y. Jiang, H. Xu, Y. Zhang, B. Yang, Y. Sun, H. H. Hng, N. Lu, L. Chi, X. Chen, *Nanoscale* **2013**, 5, 12383.
[47] H. Park, D. Shin, G. Kang, S. Baek, K. Kim, W. J. Padilla, *Adv. Mater.* **2011**, 23, 5796.
[48] Y. Hou, B. L. Abrams, P. C. Vesborg, M. E. Bjorketun, K. Herbst, L. Bech, A. M. Setti, C. D. Damsgaard, T. Pedersen, O. Hansen, J. Rossmeisl, S. Dahl, J. K. Norskov, I. Chorkendorff, *Nat. Mater.* **2011**, 10, 434.
[49] S. Mubeen, J. Lee, N. Singh, S. Kramer, G. D. Stucky, M. Moskovits, *Nat. Nanotechnol.* **2013**, 8, 247.
[50] J. Lee, S. Mubeen, X. Ji, G. D. Stucky, M. Moskovits, *Nano Lett.* **2012**, 12, 5014.
[51] V. Greanya, *Bioinspired photonics : optical structures and systems inspired by nature*, Boca Raton : CRC Press, Taylor & Francis Group, [2016], **2016**.
[52] P. Simonis, J. P. Vigneron, *Phys. Rev. E Stat. Nonlin. Soft Matter Phys.* **2011**, 83, 011908.
[53] V. Welch, V. Lousse, O. Deparis, A. Parker, J. P. Vigneron, *Phys. Rev. E Stat. Nonlin. Soft Matter Phys.* **2007**, 75, 041919.
[54] A. Imhof, W. L. Vos, R. Sprik, A. Lagendijk, *Phys. Rev. Lett.* **1999**, 83, 2942.
[55] J. I. L. Chen, G. von Freymann, S. Y. Choi, V. Kitaev, G. A. Ozin, *Adv. Mater.* **2006**, 18, 1915.
[56] X. Shi, Z. Lou, P. Zhang, M. Fujitsuka, T. Majima, *ACS Appl. Mater. Interfaces* **2016**, 8, 31738.
[57] C. T. Dinh, H. Yen, F. Kleitz, T. O. Do, *Angew. Chem. Int. Ed. Engl.* **2014**, 53, 6618.
[58] K. Kim, P. Thiyagarajan, H. J. Ahn, S. I. Kim, J. H. Jang, *Nanoscale* **2013**, 5, 6254.
[59] L. Zhang, C. Y. Lin, V. K. Valev, E. Reisner, U. Steiner, J. J. Baumberg, *Small* **2014**, 10, 3970.
[60] X. Zhang, Y. Liu, S.-T. Lee, S. Yang, Z. Kang, *Energ. Environ. Sci.* **2014**, 7, 1409.
[61] Z. Zhang, L. Zhang, M. N. Hedhili, H. Zhang, P. Wang, *Nano Lett.* **2013**, 13, 14.
[62] J. Cai, J. Huang, Y. Lai, *J. Mater. Chem. A* **2017**, 5, 16412.
[63] M. Law, L. E. Greene, J. C. Johnson, R. Saykally, P. Yang, *Nat. Mater.* **2005**, 4, 455.
[64] Y. Li, X. Wei, B. Zhu, H. Wang, Y. Tang, T. C. Sum, X. Chen, *Nanoscale* **2016**, 8, 11284.
[65] J. Bu, J. Fang, W. R. Leow, K. Zheng, X. Chen, *RSC Adv.* **2015**, 5, 103895.
[66] X. Zhang, Y. Liu, Z. Kang, *ACS Appl. Mater. Interfaces* **2014**, 6, 4480.
[67] Y. C. Yen, J. A. Chen, S. Ou, Y. S. Chen, K. J. Lin, *Sci Rep* **2017**, 7, 42524.

[68] J. Xu, Z. Wang, W. Li, X. Zhang, D. He, X. Xiao, *Nanoscale Res Lett* **2017**, 12, 54.
[69] H. Hu, Z. Jiao, G. Lu, J. Ye, Y. Bi, *RSC Adv.* **2014**, 4, 31795.
[70] J. M. J. den Toonder, P. R. Onck, P. O'Brien, R. Nuzzo, *Artificial Cilia*, Royal Society of Chemistry, **2013**.
[71] D. Zhang, W. Wang, F. Peng, J. Kou, Y. Ni, C. Lu, Z. Xu, *Nanoscale* **2014**, 6, 5516.
[72] F. Peng, Q. Zhou, D. Zhang, C. Lu, Y. Ni, J. Kou, J. Wang, Z. Xu, *App. Catal. B Environ.* **2015**, 165, 419.
[73] J. Huang, L. Lin, D. Sun, H. Chen, D. Yang, Q. Li, *Chem. Soc. Rev.* **2015**, 44, 6330.
[74] M. R. Weatherspoon, Y. Cai, M. Crne, M. Srinivasarao, K. H. Sandhage, *Angew. Chem. Int. Ed. Engl.* **2008**, 47, 7921.
[75] G. Zhang, J. Zhang, G. Xie, Z. Liu, H. Shao, *Small* **2006**, 2, 1440.
[76] K. Liu, L. Jiang, *Nano Today* **2011**, 6, 155.
[77] K. Pushpavanam, S. Santra, K. Rege, *Langmuir* **2014**, 30, 14095.
[78] E. Dujardin, C. Peet, G. Stubbs, J. N. Culver, S. Mann, *Nano Lett.* **2003**, 3, 413.
[79] M. Mertig, L. Colombi Ciacchi, R. Seidel, W. Pompe, A. De Vita, *Nano Lett.* **2002**, 2, 841.
[80] J. Xie, Y. Zheng, J. Y. Ying, *J. Am. Chem. Soc.* **2009**, 131, 888.
[81] M. N. V. Ravi Kumar, *React. Funct. Polym.* **2000**, 46, 1.
[82] H. Wang, B. Zhu, X. Ma, Y. Hao, X. Chen, *Small* **2016**, 12, 2715.
[83] H. Wang, B. Zhu, H. Wang, X. Ma, Y. Hao, X. Chen, *Small* **2016**, 12, 3360.
[84] B. Zhu, H. Wang, W. R. Leow, Y. Cai, X. J. Loh, M.-Y. Han, X. Chen, *Adv. Mater.* **2016**, 28, 4250.
[85] H. Wang, Y. Du, Y. Li, B. Zhu, W. R. Leow, Y. Li, J. Pan, T. Wu, X. Chen, *Adv. Funct. Mater.* **2015**, 25, 3825.
[86] V. Greanya, *Bioinspired Photonics: Optical Structures and Systems Inspired by Nature*, CRC Press, **2015**.
[87] K. Yu, T. Fan, S. Lou, D. Zhang, *Prog. Mater. Sci.* **2013**, 58, 825.
[88] Y. Liu, J. Goebl, Y. Yin, *Chem. Soc. Rev.* **2013**, 42, 2610.
[89] G. Zan, Q. Wu, *Adv. Mater.* **2016**, 28, 2099.
[90] P. Vukusic, J. R. Sambles, C. R. Lawrence, *Nature* **2000**, 404, 457.
[91] P. Vukusic, J. R. Sambles, C. R. Lawrence, *Proc. Biol. Sci.* **2004**, 271 Suppl 4, S237.
[92] W. Zhang, D. Zhang, T. Fan, J. Gu, J. Ding, H. Wang, Q. Guo, H. Ogawa, *Chem. Mater.* **2009**, 21, 33.
[93] J. Chen, H. Su, F. Song, W. J. Moon, Y. S. Kim, D. Zhang, *J. Colloid Interface Sci.* **2012**, 370, 117.
[94] L. Ding, H. Zhou, S. Lou, J. Ding, D. Zhang, H. Zhu, T. Fan, *Int. J. Hydrogen Energy* **2013**, 38, 8244.
[95] Y. Zhang, Y. Tang, X. Liu, Z. Dong, H. H. Hng, Z. Chen, T. C. Sum, X. Chen, *Small* **2013**, 9, 996.
[96] R. Yan, M. Chen, H. Zhou, T. Liu, X. Tang, K. Zhang, H. Zhu, J. Ye, D. Zhang, T. Fan, *Sci Rep* **2016**, 6, 20001.
[97] J. A. Seabold, K. S. Choi, *J. Am. Chem. Soc.* **2012**, 134, 2186.
[98] F. F. Abdi, L. Han, A. H. Smets, M. Zeman, B. Dam, R. van de Krol, *Nat. Commun.* **2013**, 4, 2195.
[99] J. Barber, *Philos Trans A Math Phys Eng Sci* **2007**, 365, 1007.
[100] H. Zhou, T. Fan, D. Zhang, *ChemSusChem* **2011**, 4, 1344.
[101] R. F. Evert, S. E. Eichhorn, *Esau's Plant Anatomy: Meristems, Cells, and Tissues of the Plant Body: Their Structure, Function, and Development*, Wiley, **2006**.
[102] Z. Schnepp, W. Yang, M. Antonietti, C. Giordano, *Angew. Chem. Int. Ed. Engl.* **2010**, 49, 6564.
[103] J. Liu, Q. Yang, W. Yang, M. Li, Y. Song, *J. Mater. Chem.* **2013**, 1, 7760.

[104] X. Li, T. Fan, H. Zhou, S.-K. Chow, W. Zhang, D. Zhang, Q. Guo, H. Ogawa, *Adv. Funct. Mater.* **2009**, 19, 45.
[105] H. Zhou, L. Ding, T. Fan, J. Ding, D. Zhang, Q. Guo, *App. Catal. B Environ.* **2014**, 147, 221.
[106] H. Zhou, J. Guo, P. Li, T. Fan, D. Zhang, J. Ye, *Sci Rep* **2013**, 3, 1667.
[107] Z. Jiang, D. Liu, D. Jiang, W. Wei, K. Qian, M. Chen, J. Xie, *Dalton Trans.* **2014**, 43, 13792.
[108] T. Klaus, R. Joerger, E. Olsson, C. G. Granqvist, *Proc. Natl. Acad. Sci.* **1999**, 96, 13611.
[109] J. L. Gardea-Torresdey, K. J. Tiemann, G. Gamez, K. Dokken, S. Tehuacanero, M. José-Yacamán, *J. Nanopart. Res.* **1999**, 1, 397.
[110] M. B. Dickerson, K. H. Sandhage, R. R. Naik, *Chem. Rev.* **2008**, 108, 4935.
[111] Z. Shen, B. Liu, V. Pareek, S. Wang, X. Li, L. Liu, S. Liu, *RSC Adv.* **2015**, 5, 80488.
[112] S. Kracht, M. Messerer, M. Lang, S. Eckhardt, M. Lauz, B. Grobety, K. M. Fromm, B. Giese, *Angew. Chem. Int. Ed. Engl.* **2015**, 54, 2912.
[113] S. Zhang, H. Zhang, S. Wang, L. Liu, S. Liu, *Catal. Sci. Technol.* **2017**, 7, 4355.
[114] H. Lee, S. M. Dellatore, W. M. Miller, P. B. Messersmith, *Science* **2007**, 318, 426.
[115] J. Saiz-Poseu, J. Sedo, B. Garcia, C. Benaiges, T. Parella, R. Alibes, J. Hernando, F. Busque, D. Ruiz-Molina, *Adv. Mater.* **2013**, 25, 2066.
[116] M. Lee, J. U. Kim, J. S. Lee, B. I. Lee, J. Shin, C. B. Park, *Adv. Mater.* **2014**, 26, 4463.
[117] C. Wang, Y. Wu, J. Lu, J. Zhao, J. Cui, X. Wu, Y. Yan, P. Huo, *ACS Appl. Mater. Interfaces* **2017**, 9, 23687.
[118] T. N. Reddy, J. Manna, R. K. Rana, *ACS Appl. Mater. Interfaces* **2015**, 7, 19684.
[119] T. N. Reddy, G. Begum, R. K. Rana, *Phys. Chem. Chem. Phys.* **2017**, 19, 7624.
[120] S. Chen, T. Takata, K. Domen, *Nat. Rev. Mater.* **2017**, 2, 17050.
[121] J. P. Giraldo, M. P. Landry, S. M. Faltermeier, T. P. McNicholas, N. M. Iverson, A. A. Boghossian, N. F. Reuel, A. J. Hilmer, F. Sen, J. A. Brew, M. S. Strano, *Nat. Mater.* **2014**, 13, 400.
[122] K. K. Sakimoto, A. B. Wong, P. D. Yang, *Science* **2016**, 351, 74.
[123] X. Wang, C. Liow, D. Qi, B. Zhu, W. R. Leow, H. Wang, C. Xue, X. Chen, S. Li, *Adv. Mater.* **2014**, 26, 3506.
[124] X. Wang, C. Liow, A. Bisht, X. Liu, T. C. Sum, X. Chen, S. Li, *Adv. Mater.* **2015**, 27, 2207.
[125] L. Jiang, Y. Sun, F. Huo, H. Zhang, L. Qin, S. Li, X. Chen, *Nanoscale* **2012**, 4, 66.

Figure 1. Overview of bio-inspired plasmonic photocatalyst. Antireflective, 3D photonic and hieratical biostructures are employed to improve catalytic efficiency by biomaterial assisted synthesis.

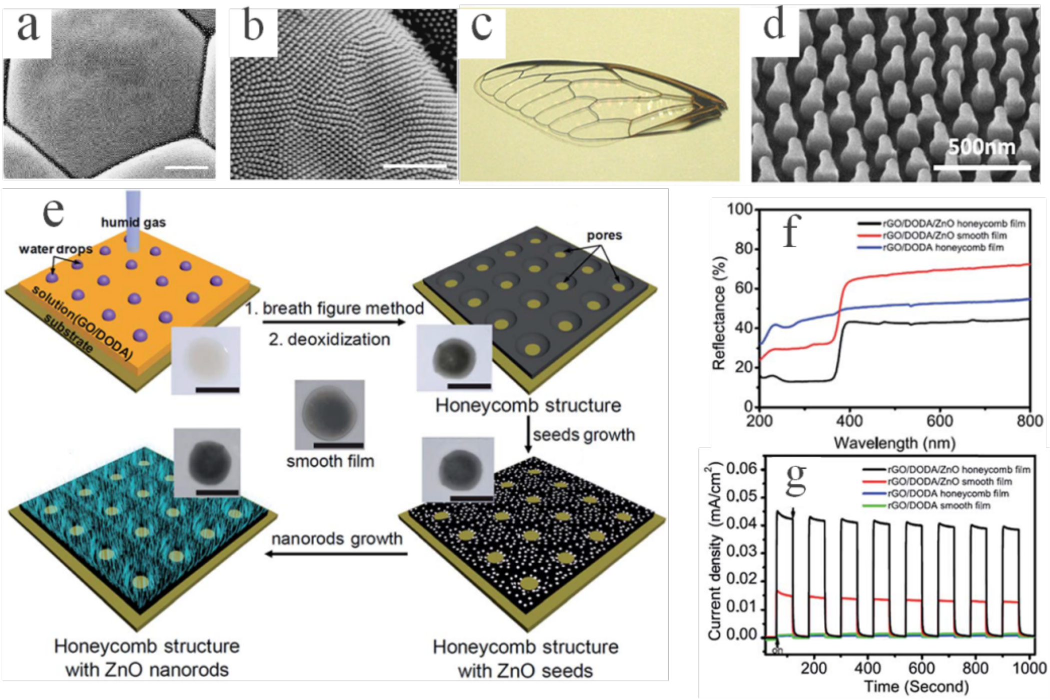

Figure 2. a, b) SEM image of highly ordered moth eye nipple nanostructures on the corneal surface. Reproduced with permission.[37] Copyright 2006, The Royal Society. c) Photographic image and d) tilted top view SEM image of Cicada wing. Reproduced with permission.[39] Copyright 2015, American Chemical Society. e) Schematic representation of the preparation of a rGO/DODA/ZnO honeycomb film. Images in clock direction corresponding to: preparation honeycomb film, reduction of honeycomb film by hydrazine vapor, coating of ZnO seeds on honeycomb film, growth of ZnO NRs honeycomb film (inset shows the corresponding sample photographs of each step. f) Reflectance spectra of rGO/DODA/ZnO smooth film (red), rGO/DODA honeycomb film (blue), and rGO/DODA/ZnO honeycomb film (black), respectively g) Photocurrent versus time under chopped irradiation of rGO/DODA/ZnO honeycomb film (black), rGO/DODA/ZnO smooth film (red), rGO/DODA honeycomb film (blue), and rGO/DODA smooth film (green) at a bias voltage of 0 V (vs. Ag/AgCl). Reproduced with permission.[43] Copyright 2015, American Chemical Society. Scale bar in (a) 5µm, (b) 2µm, (d) 500 nm, (e) 1 cm.

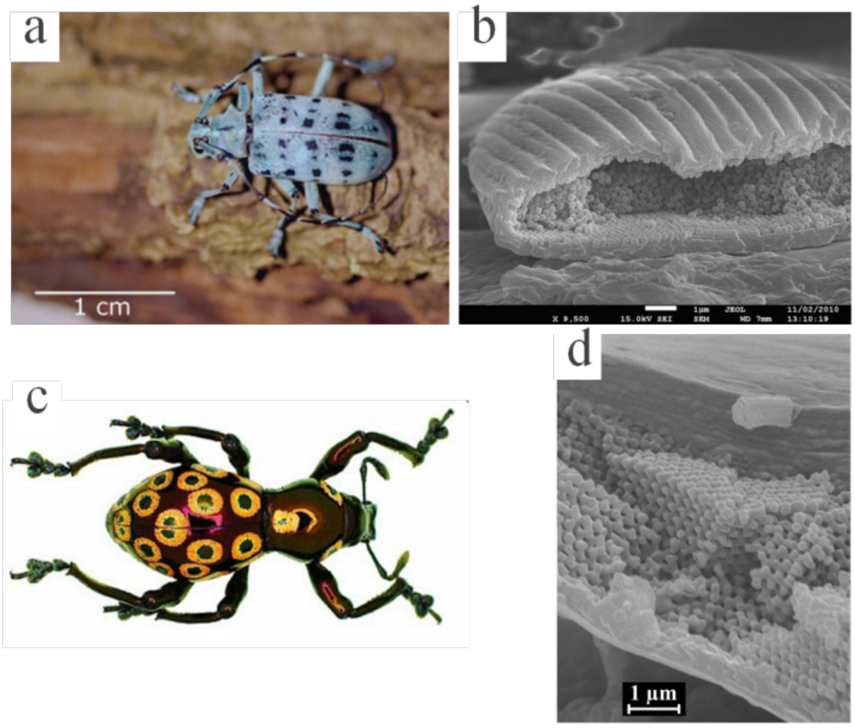

Figure 3. a) Photographic image of bright blue longhorn beetle (*Pseudomyagrus waterhousei*). The blue coloration appears diffuse and lacks iridescence. b) Corss section SEM image of a randomly selected part on one of the elytra of the longhorn beetle. The scale has an external cortex filled with a regular arrangement of monodispersed chitin spherules. Reproduced with permission.[52] Copyright 2011, American Physical Society. c) Photographic image darkly colored weevil (*Pachyrrhynchus congestus pavonius*), bearing highly conspicuous orange annular spots on the dorsal and lateral sides of its thorax and abdomen. d) Scanning electron microscope image of the internal structure of a scale, showing the layered photonic organization containing one hole and one protrusion. Reproduced with permission.[53] Copyright 2007, American Physical Society. Scale bar in (a) 1 cm, (b,c) 1µm.

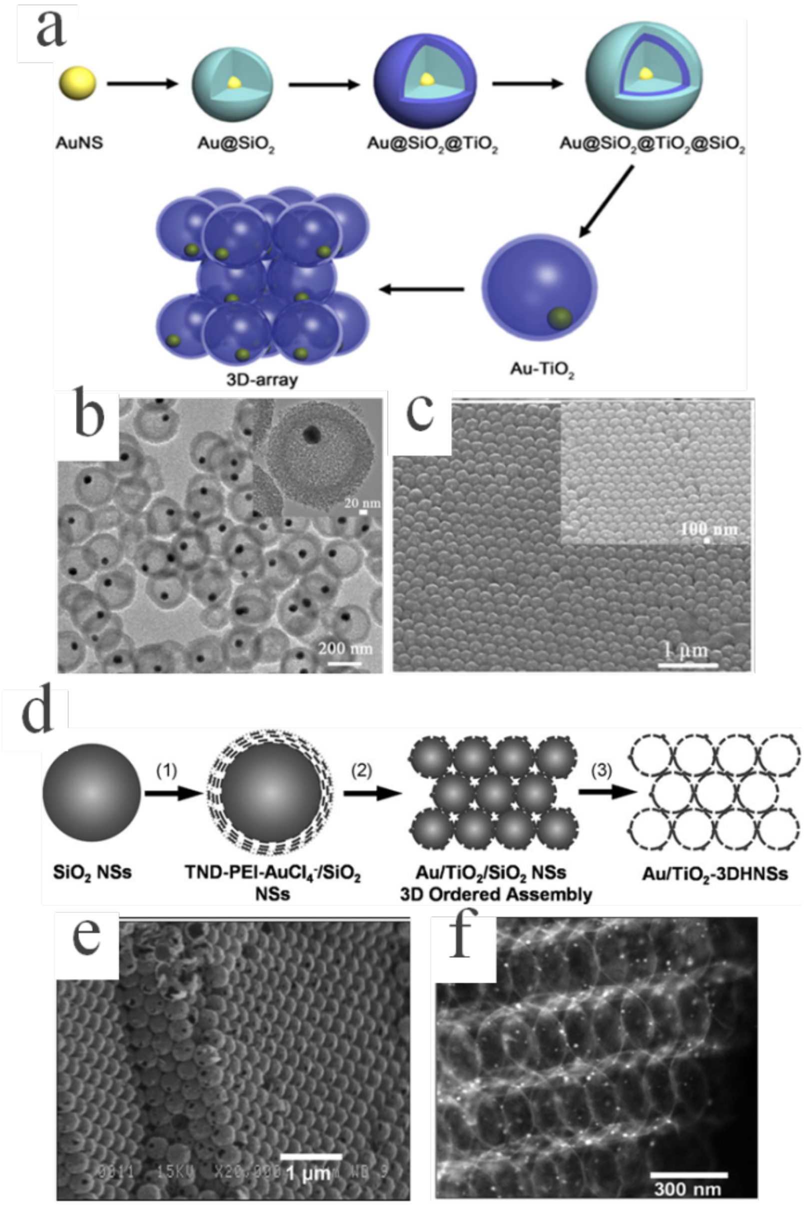

Figure 4. a) Schematic illustration of Synthesizing Au-TiO_2 and 3D-array. b) TEM image of Au-TiO_2, inset image is the enlarged one Au-TiO_2. c) SEM top-view images of 3D-array, inset is the enlarged image. Reproduced with permission.[56] Copyright 2016, American Chemical Society. d) Schematic illustration of the procedure for the prepare of Au/TiO_2-3DHNSs: 1) uniform coating of TNDs on the surface of colloidal SiO_2 NSs and loading of $AuCl^{4-}$; 2) assembly into a 3D ordered structure followed by calcination; 3) removal of SiO_2 to obtain Au/TiO_2-3DHNSs. e) SEM image f) HRTEM image of Au/TiO_2-3DHNSs. Reproduced with permission. [57] Copyright 2014, Wiley-VCH. Scale bar in (b) 200 nm, inset 20 nm, (c) 1 μm inset 100 nm, (e) 1μm, (f) 300 nm.

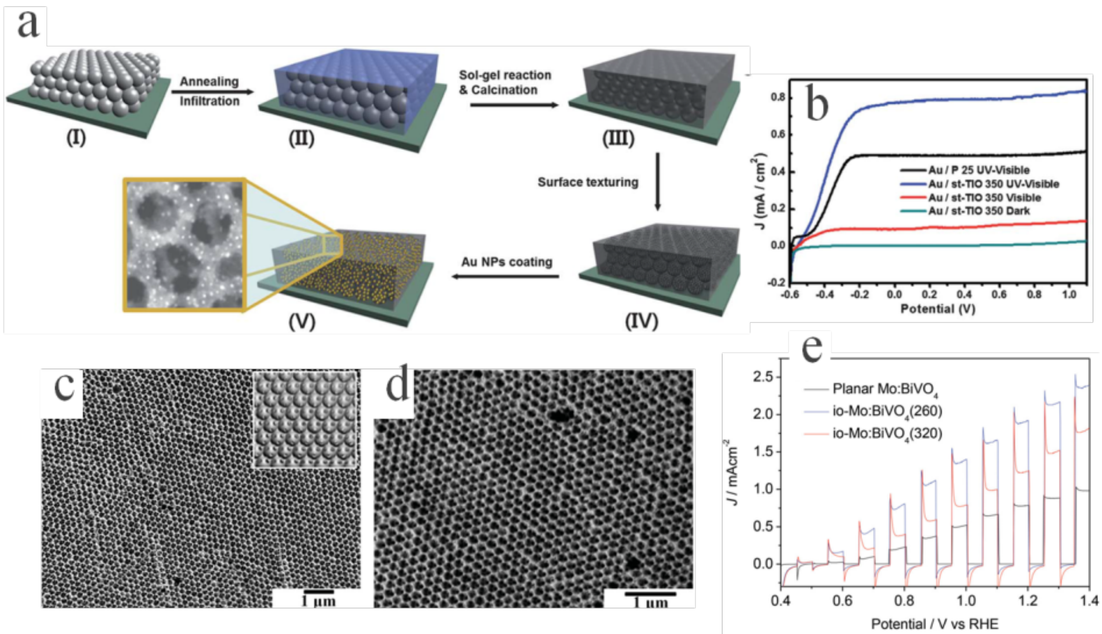

Figure 5. a) Schematic illustration of the fabrication process for a Au/st-TIO structure. (I) Self-assembly of PS; (II) assembly of PS infiltrated by $TiCl_4$ solutions; (III) removal of PS and sol-gel reaction of TiO_2 precursors; (IV) selective removal one domain in the triblock copolymer film; (V) hydrothermal deposition of Au NPs on st-TIO.b) I-V curve of Au/P-25 under UV-visible light illumination and Au/st-TIO structures under UV-visible, visible light illumination, and dark conditions. Reproduced with permission. [58] Copyright 2013, The Royal Society of Chemistry. c, d) SEM images of io-Mo:$BiVO_4$ prepared from colloidal crystal templates of polystyrene spheres with c) 260 nm diameter and d) 320 nm diameter. e) Linear sweep voltammogram curves of the control, 260 and 320 nm template fabricated film under chopped illumination. Reproduced with permission.[59] Copyright 2014, Wiley-VCH. Scale bar in (c) 1μm, (d) 1μm.

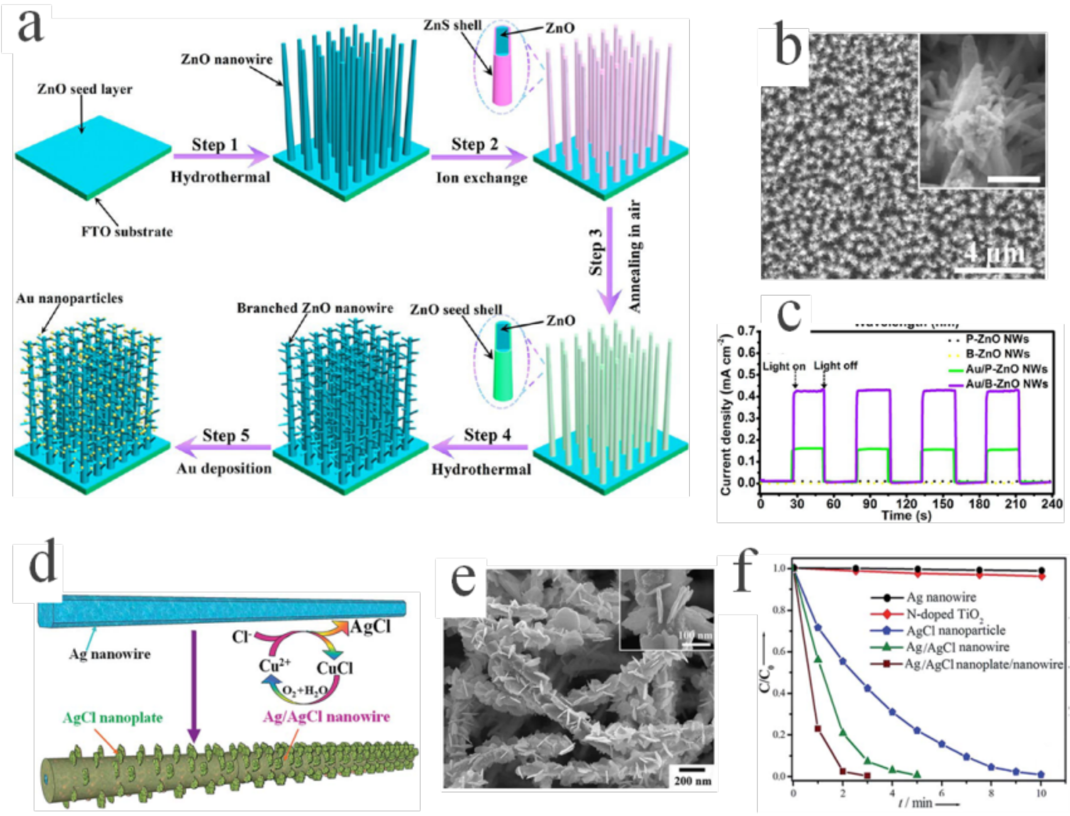

Figure 6. a) Schematic illustration of the processes to fabricate Au NPs modified B-ZnO NWs arrays photoelectrode. b) Top-view SEM images of Au NPs modified B-ZnO NWs arrays. c) Chronoamperomertic I-t curves collected at 1 V vs RHE with repeated on/off cycles of simulated sunlight coupled with a 420 nm long-wave-pass filter. Reproduced with permission.[66] Copyright 2014, American Chemical Society. d) Schematic illustrations for the growth process of Ag/AgCl nanoplate–nanowire hierarchical structures by reacting Ag nanowires and $CuCl_2$ at room temperature. e) SEM images of AgCl nanoplate-Ag/AgCl nanowire hierarchical structures. f) Photocatalytic activities of Ag/AgCl nanoplate-nanowire hierarchical structures for RhB degradation under visible-light irradiation. Scale bar in (b) 4μm, inset 200 nm (e) 200 nm, inset 100 nm. Reproduced with permission. [69] Copyright 2014, The Royal Society of Chemistry.

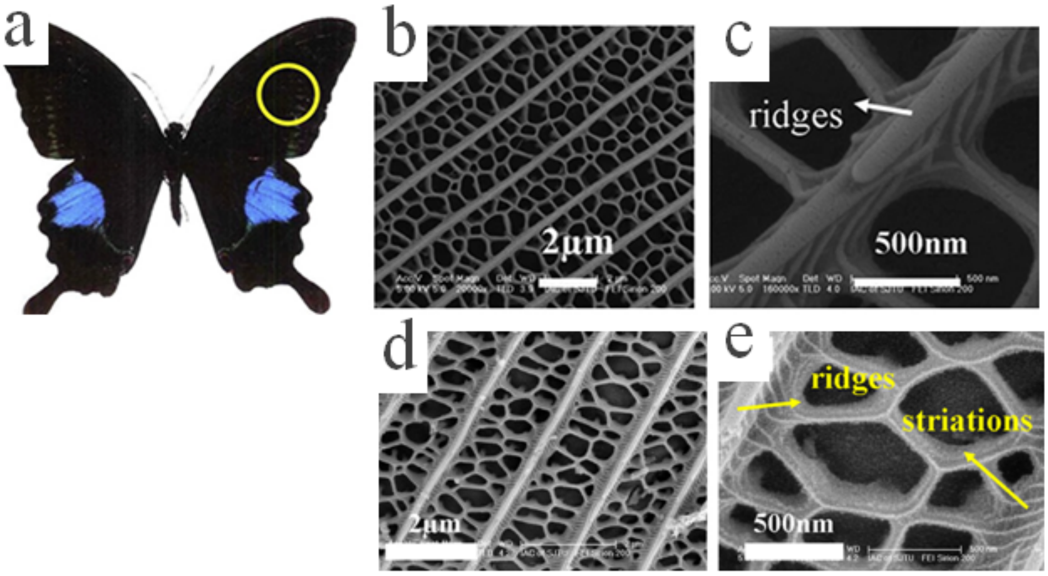

Figure 7. a) Photograph of the *Papilio Paris* butterfly. b, c) FESEM images of the butterfly wing's black areas. d, e) FESEM images of replacated biomorphic wing structure by Au/TiO_2. Reproduced with permission.[93] Copyright 2011, Elsevier Inc.. Scale bar in (b, d) 2 µm, (c, e) 500 nm.

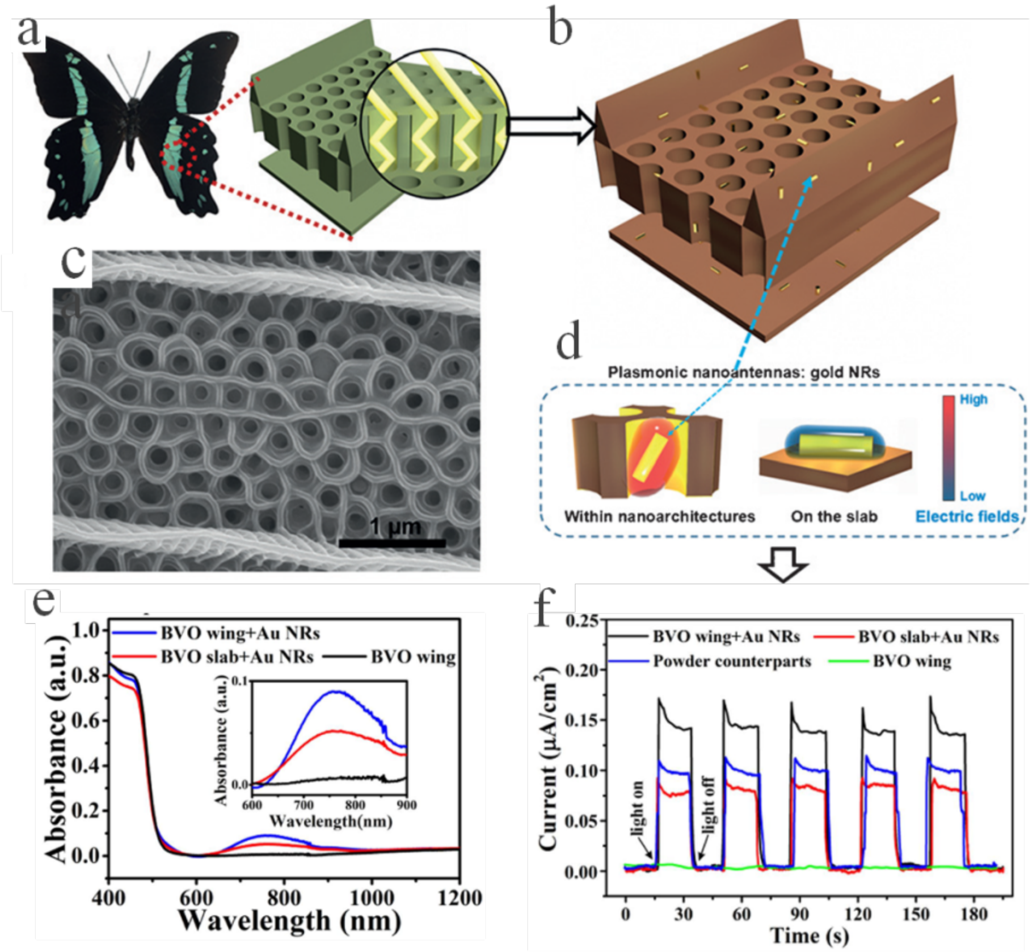

Figure 8. a) The image of butterfly wing and microstructural model. b) Light-harvesting plasmonic Au-NRs loaded onto a typical photocatalytic unit with biological 3D architectures. c) SEM top view of butterfly-wing. d) Illustration of structure-enhanced LSPR-induced electric fields by the comparison between Au NRs within nanoarchitectures and Au NRs on the slab. e) Optical absorption of Au-NRs loaded butterfly wing structural made by BVO. f) Photocurrent response of BVO+Au NRs series under chopped monochromatic light at 750 nm. Reproduced with permission.[96] Copyright 2016, Nature Publishing Group. Scale bar in (c) 1μm.

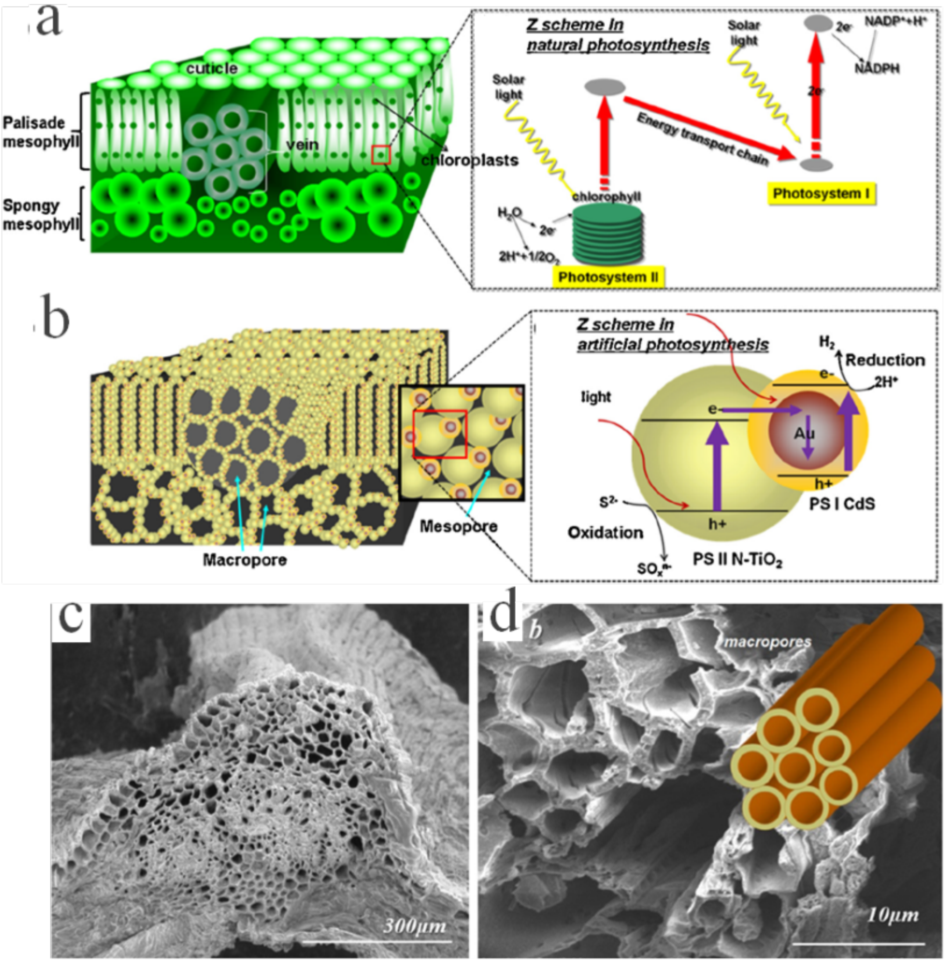

Figure 9. a) Schematic illustrations of plant leafs hierarchical morphologies (left) and Z scheme in natural photosynthesis (right). b) The cross section of the hierarchical macro/mesoporous heterostructures in the multicomponent artificial systems (left) and Z scheme in artificial photosynthesis (right). c) FESEM image of the cross-section of the vein architecture of *Cherry blossom* leaf. d) TEM image of the layered nanostructure of thylakoid membranes.inset is a schematic illustration. Reproduced with permission.[105] Copyright 2013, Elsevier B.V..

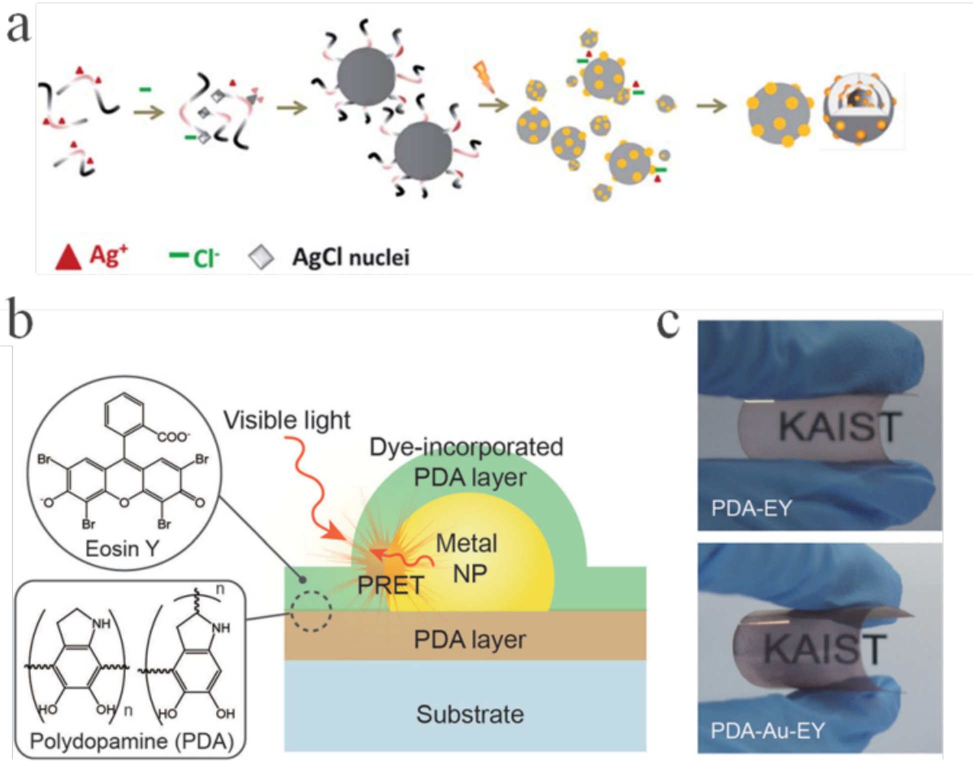

Figure 10. a) Mechanisms for biogenic Ag@AgCl plasmonic nanohybrid formation within LB broth through photo-induced and accelerated ripening process. Reproduced with permission.[111] Copyright2015, The Royal Society of Chemistry. b) Schematic illustration of mussel-inspired PDA plasmonic nanohybrid for light harvesting. PDA film enables formation of core-shell nanostrucof metal NPs and photosensitizers. Eosin Y was used as biocatalyst. c) Photographs of nano hybrid films formed on flexible substrates. Reproduced with permission.[116] Copyright 2014, WILEY-VCH.

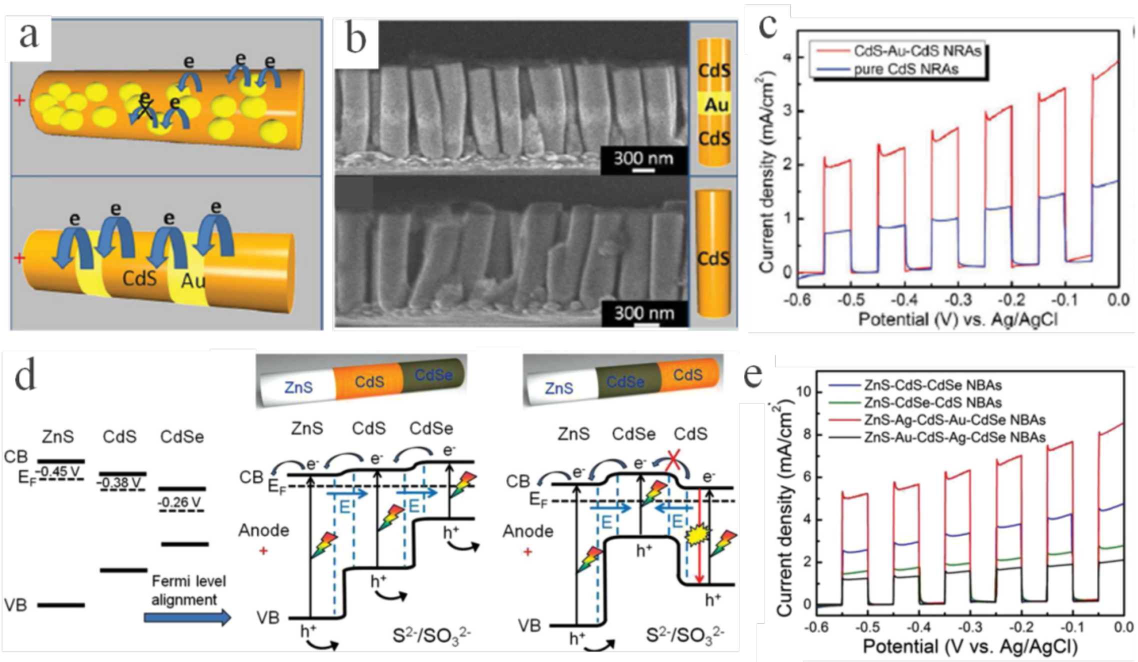

Figure 11. a) The schematic diagram of semiconductor NR loaded with plasmonic nanoparticles, up image random loaded, down image multi-segmented CdS-Au NR. b) SEM images of the side view of CdS-Au-CdS NRAs. c) Linear sweep voltammogram curves of the pure CdS NRAs and the CdS-Au-CdS NRAs. Reproduced with permission.[123] Copyright 2014, WILEY-VCH. d) Schematic llustration of the Fermi level alignment and the interfacial PICT processes for ZnS-CdS-CdSe NB, and ZnS-CdSe-CdS NB after heterostructuring. e) Linear sweep voltammogram curves of the ZnS-CdS-CdSe NBAs, ZnS-CdSe-CdS NBAs, ZnS-Ag-CdS-Au-CdSe NBAs, and ZnS-Au-CdS-Ag-CdSe NBAs. All sweep curves carried out at a scan rate of 10 mV s^{-1} at applied potentials from –0.6 to 0 V (vs Ag/AgCl), under AM 1.5 illumination of 100 mW cm^{-2}. Reproduced with permission. [124] Copyright 2015, WILEY-VCH.

Author biographs

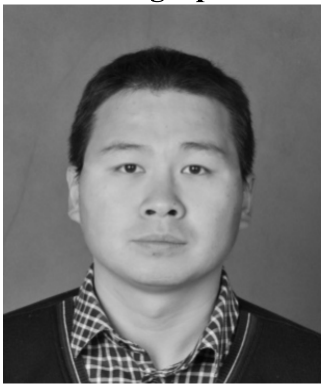

Zhihua Liu received his B.S. in chemistry from Sichuan University (P. R. China) in 2006 and Ph.D. in physical chemistry from The Chinese Academy of Sciences in 2011. Then he joined University of Twente, Netherland as a Postdoctoral Fellow, working on the fabrication of hybrid nanoelectronic device. Since 2016, he joined the group of Prof. Xiaodong Chen at Nanyang Technological University as a Postdoctoral Fellow. His current research interests include bio-inspired light manipulation device fabrication, organic spintronic device fabrication.

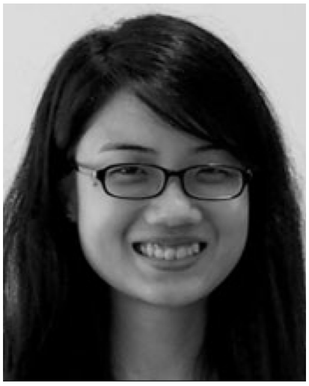

Wan Ru Leow has been a doctoral student in the School of Materials Science and Engineering at Nanyang Technological University, Singapore, since 2012. She received her B.Eng. degree in Chemical and Biomolecular Engineering in 2012. Her current research focuses on the synthesis of photocataly tic materials and flexible devices for energy conversion and storage.

Xiaodong Chen is a Professor at Nanyang Technological University, Singapore. He received his B.S. degree in chemistry from Fuzhou University (China) in 1999, M.S. degree in physical chemistry from the Chinese Academy of Sciences in 2002, and Ph.D. degree in biochemistry from the University of Muenster (Germany) in 2006. After working as a postdoctoral fellow at Northwestern University (USA), he started his independent research career as a Singapore National Research Foundation Fellow and Nanyang Assistant Professor at Nanyang Technological University in 2009. He was promoted to Associate Professor in 2013 and Full Professor in 2016. His research interests include mechanomaterials for flexible electronics, energy conversion and nano–bio interfaces.

Inspired by the delicate design in biologic systems, plasmonic photocatalyst with hierarchical structure could facilitate the rapid enhancement of photocatalytic efficiency under visible light irradiation. It increased the prospect to use full spectrum of sunlight for environmental and energy related applications such as water splitting, pollutant treatment and carbon dioxide reduction.

plasmonic photocatalyst, bio-inspired material, bio-templated synthesis, bio-inspired light manipulation

Zhihua Liu, Wan Ru Leow and Xiaodong Chen*

Bio-inspired plasmonic photocatalysts